LA-UR- 01-3581

Approved for public release; distribution is unlimited.

Title: Spatial Distribution and Interaction of Defects in Spinel, Based on Optical Studies of X-ray Irradiation Induced Processes.

Author(s): Vasyl T. Gritsyna, Kharkiv National Laboratory
Yurij G. Kazarinov, Kharkiv National Laboratory
Volodymyr A. Kobyakov, Kharkiv National Laboratory
Kurt E. Sickafus, MST-08

Submitted to: To be presented at PRICM-4: Fourth Pacific Rim International Conference on Advanced Materials and Processing, Honolulu, Hawaii, Dec. 11-15, 2001

Spatial Distribution and Interaction of Defects in Spinel, Based on Optical Studies of X-ray Irradiation Induced Processes

Vasyl T. Gritsyná, Yurij G. Kazarinov, Volodymyr A. Kobyakov and Kurt E. Sickafus

Kharkiv National University, Kharkiv 61077, Ukraine
Los Alamos National Laboratory, Los Alamos NM 87545, USA

Kinetic studies of optical center accumulation and decay, together with the growth and decay of radioluminescence (RL) in magnesium aluminate spinel $MgAl_2O_4$, were performed at room temperature. We observed two stages of defect accumulation during prolonged X-ray irradiation, as evidenced by changes in absorption bands at 3.78 and 4.15 eV related to antisite defects, and bands at 4.75 and 5.3 eV due to F-type centers. A correlation was found between optical absorption band growth and the intensities of RL bands at 4.86 and 5.02 eV, the latter of which originate from electron-hole recombination processes. The rate of decay of absorption centers and RL intensities is dependent on time after X-ray irradiation. also Both decay rates could be described by a two-stage exponential law. Results are discussed using a model that includes tunneling and recombination of electron and hole centers on spatially correlated defects located at different distances from one another.

Keywords: magnesium aluminate spinel ($MgAl_2O_4$), optical absorption, radioluminescence, kinetics

1. Introduction

Magnesium aluminate spinel ($MgAl_2O_4$) has been proposed as a potential optical and insulation material for use in nuclear fusion reactors, since it possesses excellent radiation resistance properties [1]. The high tolerance of spinel can have several origins such as the high concentration of structural vacancies in spinel, difficulties in forming clusters of point defects, or high degrees of cation disorder [2,3]. Therefore, the nature and initial state of defects in spinel crystals can play an important role in the behavior of this material under irradiation.

The unit cell of $MgAl_2O_4$ spinel consists of a face-centered cubic lattice of 32 oxygen ions and 64 tetrahedral and 32 octahedral interstices between these anions. In normal spinel crystals, Mg^{2+} ions occupy 1/8 of the tetrahedral interstices, while Al^{3+} ions occupy 1/2 of the octahedral positions. It is known that spinel crystals grown under laboratory conditions are partially inverse, i.e. up to 0.3 Al^{3+} ions per unit cell occupy tetrahedral sites and equal part of Mg^{2+} are placed in octahedral positions, producing so-called antisite defects. Synthetic crystals also unavoidably contain impurity ions of different charges and sizes, such as Fe, Mn, Cr; these species replace constituent ions in different ways and lead to the formation of ional lattice defects.

There are a variety of intrinsic defects in spinel, including anion and cation vacancies, antisite defects, and point defect complexes. Ionizing irradiation creates free charge carriers and leads to the formation of optically active centers that reside on these intrinsic defects. Due to the large variety of intrinsic defects, we anticipate the existence of different configurations and spatial distributions for electron and hole centers. In this paper, we present results from kinetic studies of optical absorption and radioluminescence (RL) during and after prolonged X-ray irradiation. Our goal is to gain insight into the spatial distribution and interaction of defects and impurity ions in spinel crystals.

Experimental procedure

Single crystals of stoichiometric magnesium aluminate spinel ($MgO{\cdot}1.0Al_2O_3$) were grown by the Verneuil method. Samples with dimensions of 10x10 mm^2 and 0.7 mm thickness were cut from single crystals and polished on both sides to an optical finish. Optical absorption was measured in the range 1.2-6.4 eV using either a single or dual beam spectrophotometer. Irradiations were performed using a Cu X-ray tube operating at 40 kV and 10 mA. RL measurements were made at room temperature in air by excitation using a Cu X-ray tube operating at 40 kV, 0.3 mA. Light emission was dispersed with SDL 1 grating spectrometer and recorded in the range 1.2-6.4 eV.

3. Experimental results

3.1. Time evolution of optical absorption

Optical absorption spectra obtained from unirradiated and X-ray irradiated spinel crystals are shown in Figure 1. Absorption *difference* curves (curves obtained by subtracting the unirradiated absorbance from the irradiated absorbance, with increasing irradiation time) show that optical absorption varies with irradiation time at several photon energies (Figure 2). To obtain the data in Fig. 2, difference spectra were fit with Gaussians for several bands, bands relating to V-type (3.1 eV) and F-type (4.75 and 5.3 eV) centers, as well as bands tentatively ascribed to optical centers on antisite defects (3.78 and 4.15 eV) [4]. The most intense bands are those identified with centers on antisite defects. These bands do not saturate, even after long irradiation times. The rate of defect accumulation, as determined by optical absorption measurements, exhibits a sublinear dependence on X-ray irradiation time. This dependence has two possible origins: (1) only a limited number of defects serve as optical centers by capturing charge carriers generated by irradiation; (2) an optical decay process occurs concurrent with the formation of optical centers. The first effect usually leads to linear growth of optical centers at low irradiation times and saturation at long times. This is not consistent with the data in Fig. 2. To test the decay process concept, we fit the accumulation curves in Fig. 2 with a simple function consisting of two exponential terms:

$$\Delta D = A_1\left(1-e^{-t/\tau_1}\right)+A_2\left(1-e^{-t/\tau_2}\right) \qquad (1).$$

For bands at 3.78 and 4.15 eV, we found the following

characteristic times: τ_1=3.0±0.2 min and τ_2=33±3 min. For bands at 4.75 and 5.3 eV, we found different characteristic times: τ_1=7.2±0.5 min and τ_2=62±5 min. The contributions of the short and long time process components can be estimated from the ratio A_1/A_2. This ratio is the same for all bands, $A_1/A_2 \sim 3$. This suggests that the optical decay process has the same origin for all bands.

Absorption spectra measured after X-ray irradiation exhibit reductions in band intensities with time. This decay process is illustrated in Figure 3 for several absorption bands. Again, it was possible to fit this experimental data with by two exponential decay components for each band:

$$\Delta D = B_1 e^{-t/t_1} + B_2 e^{-t/t_2} \quad (2)$$

For bands at 3.78 and 4.15 eV, we found the following characteristic times: t_1=10.3±0.5 min and t_2=85±5 min. However, for the band at 4.75 eV, both times are shorter: t_1=7.5±0.5 min and t_2=36±3 min.

3.2. Time evolution of radioluminescence

In our previous investigations, we found that RL spectra consist of a strong, complex UV-band at ~5 eV and additional emission at 2.38 and 1.81 eV. The complex, UV-band could be deconvoluted into two principal components with maxima at 4.86 and 5.02 eV. These are tentatively identified with recombination processes that involve optical center transformations on antisite defects. The other bands at 2.38 and 1.81 eV are related to emission centered on Mn^{2+} and Cr^{3+} impurity ions, respectively [4]. In this study, we measured the growth in intensity of different luminescence bands in the course of prolonged X-ray irradiation up to 3000 s at room temperature (Figure 4). To distinguish the contributions from the principal UV-band components (at 4.86 and 5.02 eV), we measured UV luminescence at 4.43 and 5.1 eV. This is the reason for the asterisks following the 4.86 and 5.02 eV labels in Fig. 4 and subsequent figures.

The UV-band RL intensities grow very slowly with irradiation time. Saturation of intensity was reached after X-ray irradiation for about 3000 s. This Process of evolution in RL intensity can be described by an exponential function similar to that used to describe optical absorption evolution (Eqn. 1), but the characteristic times are different: τ_1=7.3±0.5 min and τ_2=93±5 min for the 5.02 eV band, and τ_1=9.0±0.5 min and τ_2=93±5 min for the 4.86 eV band. The behavior of other two bands is quite different compared to the UV-band. These bands quickly approach saturation and after 500 s X-ray irradiation, they begin to decline with increasing irradiation time. The first stage of growth to saturation for both bands (at 2.38 and 1.81 eV) can be described using Eq. (1), with characteristics times of several seconds and several hundred seconds. But quantifying such short times of growth is made difficult due to the limited time resolution of apparatus.

After terminating X-ray irradiation at 3600 s, we examined the rate of decay of the various RL bands with time. These results are shown in Figure 5. The slow UV-band decay can again be described by an exponential expression as in Eqn. (2). We obtained the following characteristic times: for the 5.02 eV band, t_1=5.5±0.2 min and t_2=22±2 min; for the 4.86 eV band, t_1=4.63±0.3 min and t_2=37±3 min. The decay of the 2.38 and 1.81 eV bands goes much faster.

3.3. Correlation between the kinetics of optical absorption and radioluminescence

To obtain information regarding a possible correlation between the accumulation of optical absorption centers and their decay leading to luminescence processes, we plotted the time dependence for both of these physical values using a log-log scale (Figure 6). Because optical absorption bands at 3.1, 3.78, and 4.15 eV exhibit the same time dependence, we show only one of these bands (3.78 eV) in Fig. 6. Likewise, the band at 4.75 eV is not shown in Fig. 6, as it mimics the behavior of the 5.3 eV band. From Fig. 6, one can see that luminescence intensities follow the rise in the absorption bands for times greater than 100 s. The change in RL intensity versus time for impurity ions is quite different from any absorption band, however. Figure 7 combines changes in the RL intensities of UV-bands with optical density changes versus time following the termination of X-ray irradiation. In this log-log scale plot, it is apparent that each curve possesses a knee, i.e., there are distinct short time and long-time regimes. In each case, the short and long-time regimes can be fit by exponential functions with different characteristic times. It is also evident in Fig. 7 that there is correlation between the 5.02 eV RL band and the 4.75 eV absorption band; likewise for the 4.86 eV RL band and the 3.78 eV absorption band.

4. Discussion

Thermoluminescence spectra obtained in a previous investigation from X-ray irradiated spinel crystals, exhibited two prominent UV emissions at 160 and 290K [5]. Examination of depolarization spectra in spinel crystals revealed that these two peaks have a dipole origin [6]. A plausible model for dipole formation is as follows: during irradiation, antisite defects capture complementary charge carriers, i.e., a $(Al_{Mg})^+$ defect captures an electron to form neutral center, $(Al_{Mg})^0$, while a $(Mg_{Al})^-$ captures hole to form a neutral center, $(Mg_{Al})^0$. Spatially correlated electron $(Al_{Mg})^0$- and hole $(Mg_{Al})^0$-centers create dipole effects in irradiated spinel. Inverse transitions could lead to recombination luminescence. The recombination probability would depend on the distance between the paired antisite centers. The nearest pairs of centers $(Al_{Mg})^0$ and $(Mg_{Al})^0$ recombine at 160K, but centers more distantly separated centers require some activation energy for the recombination process to proceed. This explains the additional emission near room temperature (290K).

Similarly, the observed exponential decay of optical absorption with two characteristic times at room temperature indicates the existence of two different distances between the counterparts of antisite defects. In addition, the RL measurements at room temperature also reveal two long-lived decay components, indicative of a two-stage recombination process (there is also evidence for a fast decay component, but we have not attempted to model the fast decay in this study). Moreover, the characteristic times for the long-lived components of RL decay are close to the decay rates associated with optical absorption

Since we observe a strong correlation between absorption bands at 3.1, 3.78, and 4.15 eV with the 4.86 eV RL band (Fig. 7), it seem plausible to consider that an electron tunneling mechanism is in effect. This tunneling emanates f from an $(Al_{Mg})^0$ electron center to a nearly situated $(Mg_{Al})^0$ hole center, leading to emission of 4.86 eV band. Similarly, the observed correlation between the 4.75 and 5.3 eV absorption bands (related to F^+- and F-centers) with the 5.02 eV luminescence band, suggests that a process involving recombination of electron centers with V-type centers is active.

Recent calculations [6] indicate that trivalent impurities, preferentially occupy octahedral sites in spinel. The possibility to form neutrally-charged defects increases when two Al^{3+} ions replace two Mg^{2+} ions near a Mg^{2+} vacancy. In this case, one of the two Al^{3+} ions could be replaced by a Cr^{3+} or Mn^{3+} to form a defect cluster involving both antisite defects and impurity ions. Energy transfer from recombining centers on antisite defects can then induce excitation of nearby impurity ions. This mechanism may lead to delayed luminescence at 2.38 and 1.81 eV with large characteristic times.

Acknowledgment

The authors thank to Dr. T. A. Bazilevska for help in measurements of optical absorption and Ms. G. I. Bilykh for characterization of spinel samples. This research was made possible in part by Award No. UE2-2226 of the U.S. Civilian Research and Development Foundation for the Independent States of the Former Soviet Union (CRDF).

REFERENCES

1) F. W. Clinard, G. F. Hurley and L. W. Hobbs: J. Nucl. Mater., **108/109** (1982), 655-670
2) K. Fukumoto, C. Kinoshita, S. Maeda and K. Nakai: Nucl. Instr. and Meth., **B91** (1994), 252-257
3) K. E. Sickafus, et al.: J. Nucl. Mater., **219** (1995), 128-134
4) V. T. Gritsyna, I. V. Afanasyev-Charkin, V. A. Kobyakov and K. E. Sickafus: J. Am. Ceram. Soc., **82** (1999), 3365-73.
5) V. T. Gritsyna, et al.: Nucl. Instr. and Meth., **B166/167** (2000), 244-249.
6) S. S. de Sousa and A. R. Black: Rad. Eff. and Defects in Solids, **146** (1998), 123-129.

Fig. 1. Optical absorption spectra obtained from spinel crystals irradiated with X-rays for the times indicated.

Fig. 2. Optical absorption difference curves for various absorption bands (indicated by photon energy) as a function of X-ray irradiation time (results based on data in Fig. 1) .

Fig. 3. Decay in optical absorption versus time following the termination of X-ray irradiation (measured at the photon energies indicated).

Fig. 4. Growth in radioluminescence intensity as a function of X-ray irradiation time for various luminescence bands. Curves for luminescence at 4.86 and 5.02 eV are indicated by asterisks (*) because measurements were actually made at 4.43 and 5.1 eV, in an attempt to better resolve these spectral components.

Fig. 5. Decay of luminescence intensity (for various luminescence bands) versus time following termination of X-ray irradiation.

Fig. 6. Optical absorption and radioluminescence intensities versus X-ray irradiation time for various absorption and luminescence bands.

Fig. 7. Decay of optical absorption and luminescence intensities versus X-ray irradiation time for various absorption and luminescence bands, following termination of X-ray irradiation

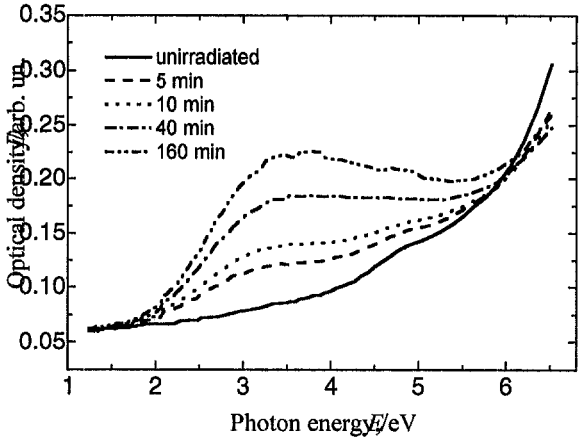

FIGURE 1

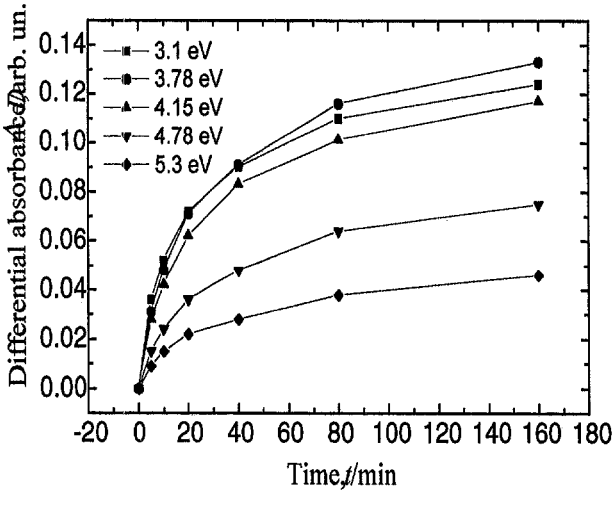

FIGURE 2

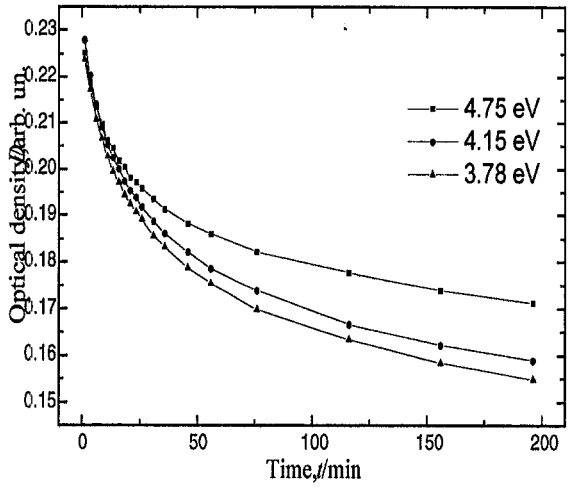

FIGURE 3

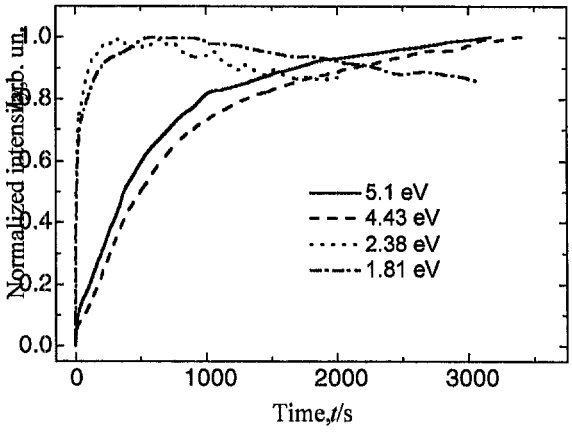

FIGURE 4

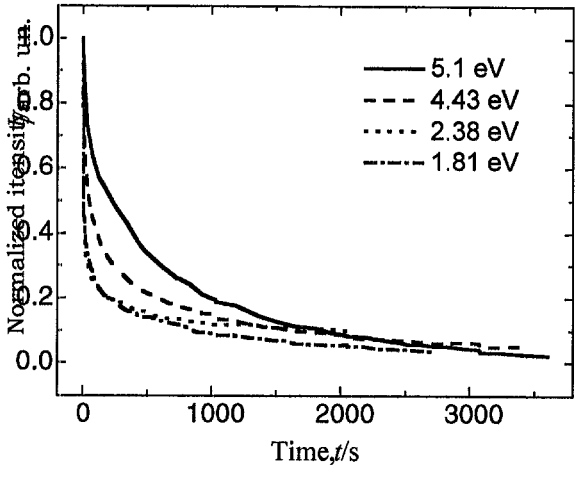

FIGURE 5

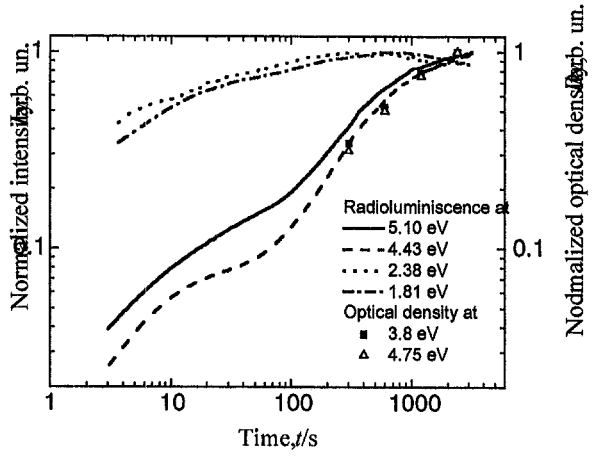

FIGURE 6

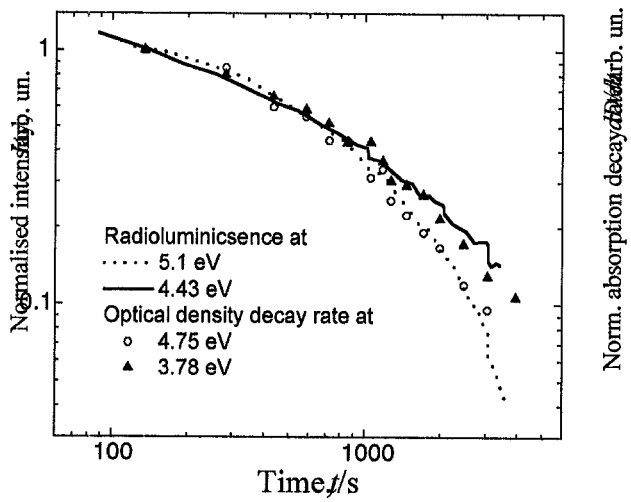
Normalised intensity, arb. un.
1
0.1
Radioluminicsence at
5.1 eV
4.43 eV
Optical density decay rate at
4.75 eV
3.78 eV
100
1000
Time, t/s
Norm. absorption decay rate, arb. un.

FIGURE 7